RESEARCH ARTICLE

WILEY

Molecular basis for covalent inhibition of glyceraldehyde-3-phosphate dehydrogenase by a 2-phenoxy-1,4-naphthoquinone small molecule

Stefano Bruno[1] | Elisa Uliassi[2] | Mirko Zaffagnini[2] | Federica Prati[2,†] | Christian Bergamini[2] | Riccardo Amorati[3] | Gianluca Paredi[1] | Marilena Margiotta[1] | Paola Conti[4] | Maria Paola Costi[5] | Marcel Kaiser[6,7] | Andrea Cavalli[2,8] | Romana Fato[2] | Maria Laura Bolognesi[2] (ORCID)

[1]Department of Pharmacy, University of Parma, Parma, Italy

[2]Department of Pharmacy and Biotechnology, Alma Mater Studiorum - University of Bologna, Bologna, Italy

[3]Department of Chemistry "G. Ciamician", Alma Mater Studiorum - University of Bologna, Bologna, Italy

[4]Department of Pharmaceutical Sciences, University of Milan, Milan, Italy

[5]Department of Life Sciences, University of Modena and Reggio Emilia, Modena, Italy

[6]Swiss Tropical & Public Health Institute, Basel, Switzerland

[7]University of Basel, Basel, Switzerland

[8]CompuNet, Istituto Italiano di Tecnologia, Genova, Italy

Correspondence
Maria Laura Bolognesi, Department of Pharmacy and Biotechnology, Alma Mater Studiorum - University of Bologna, Bologna, Italy.
Email: marialaura.bolognesi@unibo.it

Current address
Federica Prati, College of Life Sciences, Sir James Black Centre, University of Dundee, Dundee, UK

Funding information
Ministero dell'Istruzione, dell'Università e della Ricerca, Grant/Award Number: 201274BNKN; University of Bologna (Italy)

Glyceraldehyde-3-phosphate dehydrogenase (GAPDH) has recently gained attention as an antiprotozoan and anticancer drug target. We have previously identified 2-phenoxy-1,4-naphthoquinone as an inhibitor of both *Trypanosoma brucei* and human GAPDH. Herein, through multiple chemical, biochemical, and biological studies, and through the design of analogs, we confirmed the formation of a covalent adduct, we clarified the inhibition mechanism, and we demonstrated antitrypanosomal, antiplasmodial, and cytotoxic activities in cell cultures. The overall results lent support to the hypothesis that 2-phenoxy-1,4-naphthoquinone binds the GAPDH catalytic cysteine covalently through a phenolate displacement mechanism. By investigating the reactivity of 2-phenoxy-1,4-naphthoquinone and its analogs with four GAPDH homologs, we showed that the covalent inhibition is not preceded by the formation of a strong non-covalent complex. However, an up to fivefold difference in inactivation rates among homologs hinted at structural or electrostatic differences of their active sites that could be exploited to further design kinetically selective inhibitors. Moreover, we preliminarily showed that 2-phenoxy-1,4-naphthoquinone displays selectivity for GAPDHs over two other cysteine-dependent enzymes, supporting its suitability as a warhead starting fragment for the design of novel inhibitors.

KEYWORDS
glyceraldehyde-3-phosphate dehydrogenase, naphthoquinones, covalent inhibition

1 | INTRODUCTION

Glyceraldehyde-3-phosphate dehydrogenase (GAPDH, EC 1.2.1.12) is the glycolytic enzyme that reversibly catalyzes the conversion of glyceraldehyde-3-phosphate (G3P) to 1,3-bisphosphoglyceric acid (BPGA) in the presence of nicotinamide adenine dinucleotide (NAD$^+$) and inorganic phosphate.[1–4] The catalytic mechanism consists of two steps: (i) the nucleophilic attack of the catalytic cysteine of the active site on the aldehyde group of G3P, followed by a hydride transfer to the nicotinamide ring, and (ii) the phosphorolysis of the thioester by inorganic phosphate (Figure 1a). The conformational transition at the active site during catalysis has been observed crystallographically.[5] The reactivity of the catalytic cysteine of GAPDH toward G3P has been ascribed to a pK_a of 6.0[6] lower than that of free thiols, such as glutathione (pK_a = 8.6),[7] and unreactive solvent-exposed cysteine residues (pK_a = 8.4).[6,8] The low pK_a reflects the involvement of the catalytic cysteine in a cysteine–histidine catalytic dyad, which provides a pK_a-lowering microenvironment that stabilizes the thiolate species.[6,9] Consistently with its distinctive pK_a, the catalytic cysteine of GAPDHs was shown to react with several chemically diverse electrophiles, such as iodoacetic acid,[1] acrylonitrile,[10] N-acetyl-p-benzoquinone imine,[11] vinyl sulfones,[12] 9,10-phenanthrenequinone,[13] and 3-bromo-isoxazoline.[14,15]

GAPDH has received considerable attention as a potential drug target.[16] Particularly, GAPDHs from protozoan parasites have been validated as suitable molecular targets for antiparasitic drugs, as several pathogenic protozoa entirely depend on glycolysis as the source of ATP in the host stage. For instance, the absence of the pyruvate dehydrogenase complex in the mitochondria of *Plasmodium falciparum* (*Pf*) restricts its ATP production to glycolysis,[17] an observation that prompted the structure-based drug design of *Pf*GAPDH inhibitors.[14,15] The unusual compartmentalization of glycolysis inside the specialized organelle glycosome in Trypanosoma and Leishmania suggested the development of GAPDH inhibitors for the treatment of Trypanosomatidae diseases.[18,19] The identification of several small-molecule inhibitors,[20–24] together with genetic validation by RNAi experiments,[25] has confirmed its druggability. In parallel, human GAPDH (*h*GAPDH) has emerged as an appealing target for anticancer therapy.[26] Indeed, an increased expression of *h*GAPDH in different types of cancer has been associated with enhanced glycolytic capacity, facilitating tumor progression.[26] Tumor cells mostly rely on glycolysis for ATP production (Warburg effect), making GAPDH inhibition an ideal strategy to specifically hit them with minimal systemic toxicity.[26] Indeed, the GAPDH covalent inhibitor 3-bromopyruvate has recently entered the early phases of clinical trials for cancer treatment.[27] Besides its "classical" glycolytic role,
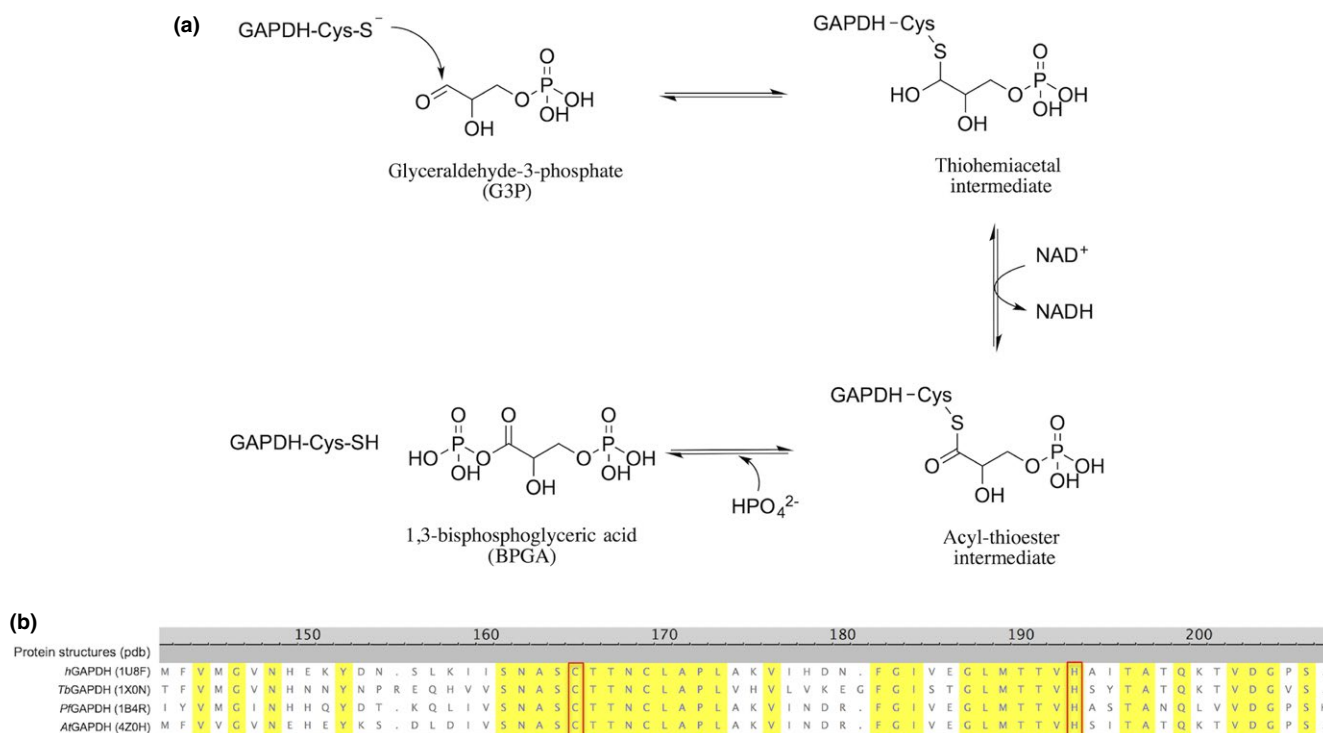

FIGURE 1 (a) Mechanism of the reaction catalyzed by GAPDH. (b) Sequence alignment of GAPDH orthologs catalytic domain used in this study using the BLAST algorithm. Conserved positions are highlighted in yellow, whereas catalytic residues are indicated by red boxes. [Colour figure can be viewed at wileyonlinelibrary.com]

a number of recent studies have demonstrated the active participation of GAPDH in several non-metabolic cellular functions, such as apoptosis,[28] transcription activation, and axonal transport.[29]

In this context, our group reported the discovery and pharmacological characterization of 2-phenoxy-naphthoquinone (**1** in Figure 1), a promising hit compound for the treatment of trypanosomiases[30] and tumors.[31] We identified **1** in a phenotypic screening as a potent inhibitor of *Trypanosoma brucei* (*Tb*) growth ($EC_{50} = 80$ nM).[30] **1** was then shown to act as *Tb*GAPDH inhibitor ($IC_{50} = 7.25$ μM) by means of chemical proteomic approaches.[32] To further validate and explore the structure–activity relationships (SAR) of this scaffold for GAPDH inhibition, we designed and synthesized a focused chemical library around **1**.[31] **1** and its 2-aryloxy-derivatives—although with flat SARs—showed to inhibit both *Tb*GAPDH[31,33] and *h*GAPDH,[31] possibly through covalent binding to the catalytic cysteine. In this respect, we speculated that **1** and its derivatives might undergo a nucleophilic substitution reaction at carbon C2 by *Tb*GAPDH catalytic cysteine, leading to phenolate displacement as leaving group and formation of the corresponding substitution adduct.[31–33] However, the exact mechanism of inhibition remains poorly understood at this time.

In this report, we investigated in depth the covalent inhibition mechanism of GAPDH inhibition by 2-phenoxy-naphthoquinones using multiple chemical, biochemical, and biological methods on GAPDH orthologs (*h*GAPDH, *Tb*GAPDH, *Pf*GAPDH, *Arabidopsis thaliana* GAPDH, *At*GAPDH). Several experimental evidences confirming a phenolate displacement mechanism were collected. We also explored the enzymatic activity profile of purposely designed chemical probes (**2–4** in Table 1) in

comparison with **1**, together with their antiparasitic and cytotoxic activities.

2 | EXPERIMENTAL SECTION

2.1 | Materials

Chemicals were of the best commercial quality available and were purchased from Sigma-Aldrich (St. Louis, MO, USA). DL-Glyceraldehyde 3-phosphate (G3P) was prepared by hydrolysis of the G3P diethyl acetal barium salt according to the manufacturer's instructions. Stocks at 34 mM concentration were stored at −20°C in small aliquots and thawed when needed.

2.2 | Protein expression and preparation

Recombinant GAPDH from *Plasmodium falciparum* (*Pf*GAPDH) was prepared as previously described.[14] Recombinant human GAPDH (*h*GAPDH) was expressed from a pET28-derived vector containing the synthetic gene (NCBI protein accession NP_001276675.1) codon-optimized for *Escherichia coli* (Geneart, Life Technologies) and then purified with conventional IMAC chromatography, similarly to *Pf*GAPDH.[14] Recombinant GAPC1 from *Arabidopsis thaliana* (*At*GAPDH) was expressed and purified as previously reported.[34] Recombinant *Trypanosoma brucei* GAPDH (*Tb*GAPDH) was expressed and purified as described in.[32] The molecular mass and purity of all proteins was determined by SDS-PAGE and the concentrations determined both spectrophotometrically and with the Bradford assay.[35] The specific activities measured with our standard assay (vide infra) were 15.2, 17, 10.6, and 23 units/mg

TABLE 1 Antitrypanosomal, antiplasmodial, and cytotoxic profile (expressed as IC_{50} (μg/ml)) of **1** and related chemical probes **2–4** and anti-*Tb*GAPDH activity

1-4
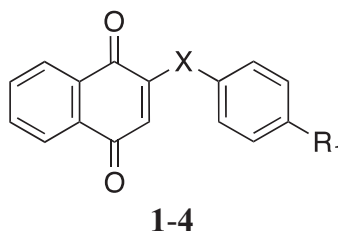
	X	R_1	*T. brucei rhodesiense* IC_{50} (μg/ml)[a,b]	*P. falciparum* IC_{50} (μg/ml)[a,b]	Cytotoxicity L6 IC_{50} (μg/ml)[a,b]	% of *Tb*GAPDH inhibition at 10 μM[b]
1	–O–	–H	0.02[c]	1.43	1.48[c]	100
2	–O–	–OMe	0.68[c]	2.41	1.71[c]	33
3	–O–	–NO₂	0.34	2.84	4.71	37
4	–NH–	–H	1.24	0.18	0.93	24

[a]IC_{50} values are the concentration of an inhibitor that causes 50% growth inhibition.
[b]IC_{50} and % of *Tb*GAPDH inhibition values are the mean of two independent determinations that varied by less than a factor of 2. The experimental error is within ±50%.
[c]Data taken from ref.[31]

for *h*GAPDH, *Pf*GAPDH, *Tb*GAPDH, and *At*GAPDH, respectively.

2.3 | Enzyme assays

GAPDH activity was monitored spectroscopically by following either the forward (glycolytic) or reverse (gluconeogenic) reactions. The oxidation of G3P was monitored using a modified version of the Ferdinand assay[36] in a buffer containing 100 mM TEA, 10 mM sodium arseniate, 5 mM EDTA, 1.5 mM NAD$^+$, and 2.8 mM G3P, at pH 7.6. GAPDHs were added at final concentrations of 30–80 nM, and NADH formation was monitored at 340 nm using a Cary4000 spectrophotometer (Agilent Technologies). The gluconeogenic reaction was measured in an assay mixture containing 50 mM Tris–HCl, 1 mM EDTA, 5 mM MgCl$_2$, 3 mM 3-phosphoglycerate, 5 units/ml of *S. cerevisiae* 3-phosphoglycerate kinase, 2 mM ATP, and 0.2 mM NADH at pH 7.5. All enzyme assays were carried out at 25°C.

2.4 | Inhibition assays

Protein inhibition by **1** was monitored both with the glycolytic and the gluconeogenic enzyme assays. For the glycolytic assays, GAPDHs (2 μM) were incubated at 25°C in a solution containing 100 mM TEA, 5 mM EDTA, 10 mM sodium arseniate at pH 7.6 in the presence of **1** at the indicated concentrations—with at least a fivefold excess. Aliquots of the reaction mixtures were periodically sampled and the residual enzyme activity measured. Aliquots of samples incubated in the absence of **1** were assayed as controls. The inactivation time–courses were fitted to monoexponential decays to obtain the apparent inactivation rates, which were then analyzed in a Kitz–Wilson double reciprocal plot,[37] obtaining a k_{inact}/K_i ratio for each inhibitor and for each GAPDH homolog. For some of these experiments, it was not possible to sample aliquots at the exact same time in replicated experiments. In these cases, at least two sets of inhibition kinetics were collected for each experiment and the statistical analysis was carried out independently on the resulting kinetic traces. The reported SEM are therefore associated with the calculated parameters rather than the raw data points.

For the inhibition assays based on the glucogenetic reaction, GAPDH homologs were incubated with **1** at indicated concentrations in solutions containing 100 mM TEA and 5 mM EDTA at pH 7.6. At different times, aliquots were sampled from the incubation mixture and assayed for enzyme activity. All inactivation experiments were monitored relative to a control sample without **1**, which was set to 100% activity at each time-point.

The reversibility of **1** inactivation was assessed by measuring GAPDH activity after 60-min treatment with **1** and after incubation for 10 min with 5 mM DTT. Protection assays by the glycolytic substrate G3P were determined by comparing the inactivation rates in the presence of 100 μM of **1** using the same conditions supplemented with 5 mM G3P. Protection by the gluconeogenic substrate BFGA was determined by adding the BPGA-generating system (3 mM 3-phosphoglycerate, 5 units/ml of 3-phosphoglycerate kinase and 2 mM ATP) to the reaction mixture where **1** was also present.

2.5 | Reaction kinetic studies

Compounds **1–3** were dissolved in methanol (final concentration 3.4×10^{-5} M), put in a quartz cuvette, and quickly mixed with an excess of dodecanthiol (0.1–0.7 mM). The increase in absorption at 413 nm (A_t) indicated the formation of the substitution product. The plots of $\ln(1 - A_t/A_{t=\infty})$ as a function of time were linear and provided the pseudo-first-order constant for the reaction of **1–3** with dodecanthiol (SH), k_{obs}. The relationship of k_{obs} on [SH] consisted of the sum of two terms: $k_{obs} = k_1$ [SH] + k_2 $(K_{SH})^{1/2}$ [SH]$^{1/2}$, accounting for the reaction of **1–3** with dodecanthiol (SH) and with dodecanthiolate (S$^-$), as [S$^-$] = $(K_{SH}$ [SH])$^{1/2}$. The values of k_2 reported in Figure 6 were obtained from the known value of K_{SH} in methanol. The results are the mean of two independent determinations that varied less by 10%.

2.6 | Mass spectrometry

The alkylation of GAPDHs by **1** was assessed by incubating the proteins (20 μM) with a 10-fold excess of **1** for 1 hr. Protein samples were then analyzed by MALDI-TOF mass spectrometry using a 4800 MALDI-TOF/TOF Analyzer (Applied Biosystems) in linear positive mode. Briefly, GAPDH samples were loaded onto the MALDI plate with the double layer method using alpha-cyano-4-hydroxycinnamic acid (CHCA) as matrix. One microlitre of 10 mg/ml CHCA in acetone was then deposited onto the MALDI plate and air-dried; a second layer was obtained by diluting 10-fold the sample with 20 mg/ml CHCA in 50% acetonitrile and 0.05% TFA. Spectra of undigested GAPDH were acquired using the linear positive mode in the 10,000–45,000 m/z range.

2.7 | Parasite growth inhibition and cytotoxicity assays

In vitro activity against bloodstream forms of *Trypanosoma brucei rhodesiense* (STIB900), chloroquine- and pyrimethamine-resistant K1 *Plasmodium falciparum* strain, and cytotoxicity assessment against L6 cells were determined as previously reported.[38]

3 | RESULTS AND DISCUSSION

3.1 | Inhibition studies of GAPDH orthologs by 1

To evaluate a possible selectivity of **1** toward GAPDHs, we investigated its inhibition on four orthologs: *h*GAPDH, *Tb*GAPDH, *Pf*GAPDH, and *At*GAPDH. Whereas the first three have been proposed as promising drug targets,[14,19,26] the molecular studies of *At*GAPDH have been particularly pursued to unveil its moonlighting role (i.e., multifunctional properties involved in a large range of biological functions besides the glycolytic one) in higher plants.[8] The alignment of the amino acid sequences of the four proteins (Figure 1b) highlights that, with the exception of the Rossmann fold of the coenzyme-binding domain and the dyad residues, no clear identities in the catalytic domains of the four enzymes are observed (Figure S1). In particular, it is difficult to localize the residues involved in the stabilization of the Ps and Pi sites, anion binding sites that have been identified in the GAPDH catalytic site as responsible for binding the C-3 phosphate of G3P and the inorganic phosphate group, respectively.[39] Thus, it is conceivable that **1** might exhibit slightly different inhibitory properties toward the four orthologs.

The inactivation kinetics of the four enzymes were determined at different concentrations of **1** and were time- and concentration-dependent. In Figure 2, representative inhibition time–courses for *h*GAPDH at different concentrations of **1** (50–200 μM) (Panel a) and inhibition time–courses for all orthologs at a fixed concentration of **1** (100 μM) (Panel b) are reported. An analysis of the plots clearly showed that the four orthologs exhibited different inactivation profiles (Figure 2b). In particular, in the presence of 100 μM **1**, *Pf*GAPDH exhibited

the fastest inactivation kinetic in comparison with the other homologs, with a $t_{1/2}$ of around 10 min; *At*GAPDH and *Tb*GAPDH were the slowest reacting isoforms, with $t_{1/2}$s around 80 min. *h*GAPDH exhibited an intermediate reactivity toward **1**, with a $t_{1/2}$ of around 40 min. The reactivity scale observed by monitoring the reversible oxidation of G3P (forward reaction, Figure 3a) closely paralleled that observed by following the reverse reaction, that is, the reduction in BPGA (Figure 3b).

Inactivation by **1** was not reversed by addition of dithiothreitol (DTT) at 5 mM concentration (Figure S2), arguing for a non-oxidative modification of the cysteine as the underlying biochemical mechanism. Indeed, being DTT a thiol-based reductant, it could be excluded that the formation of a disulfide bond involving the cysteine thiol occurs.[40] As reported for a similar experiment performed with metalloporphyrin derivatives and apocytochrome c, this might be suggestive of a thioether bond formation between **1** and the protein (vide infra).[40]

To investigate whether inactivation of GAPDH by **1** occurred as a result of interactions at the active site, substrate protection experiments were carried out. When either G3P or BPGA was added to the incubation mixtures containing **1**, they dramatically slowed down the inactivation kinetics of all isoforms (Figure 3, Panel b), suggesting a competition for the binding at the same residue, that is, the catalytic cysteine. The alternative possibility that GAPDH inactivation is associated with a **1**-mediated modification of cysteine residues other than the catalytic one—triggering an allosteric conformational change to an inactive form—cannot be ruled out. However, to the best of our knowledge, no covalent inhibitor able to selectively modify GAPDH non-catalytic cysteines
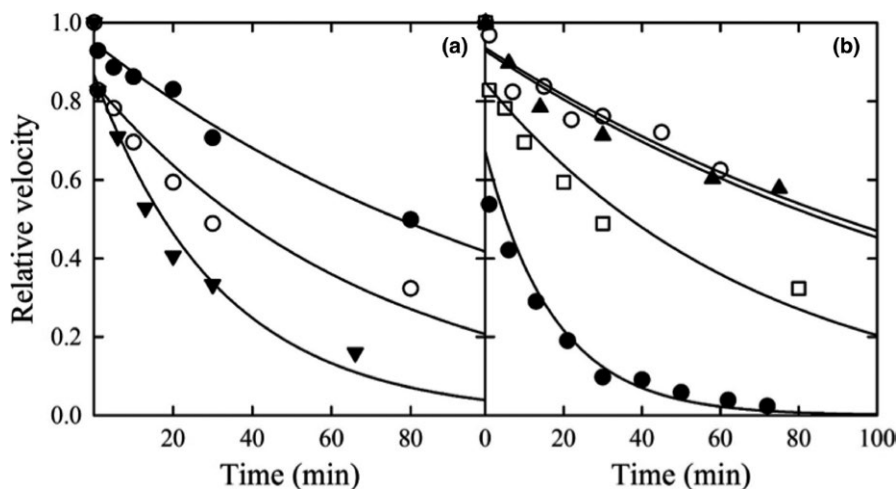

FIGURE 2 Representative time–courses of GAPDHs inactivation (forward reaction) by **1** in TEA buffer at pH 7.6. (a) Exemplary comparison of the inhibition kinetics for one of the GAPDH orthologs, *h*GAPDH, at different concentrations of **1**: 50 μM (closed circles), 100 μM (open circles), and 200 μM (closed triangles). (b) Exemplary comparison of inhibition kinetics at one concentration of **1** (100 μM) for *h*GAPDH (open squares), *Pf*GAPDH (closed circles), *At*GAPDH (closed triangles), and *Tb*GAPDH (open circles). The activities were normalized to those measured in the absence of inhibitors for each ortholog. The lines are the fittings of the experimental points to an exponential decay. Both incubation and enzyme assays were carried out at 25°C. The overall analysis of these measurements and their replicates is reported in Figure 4
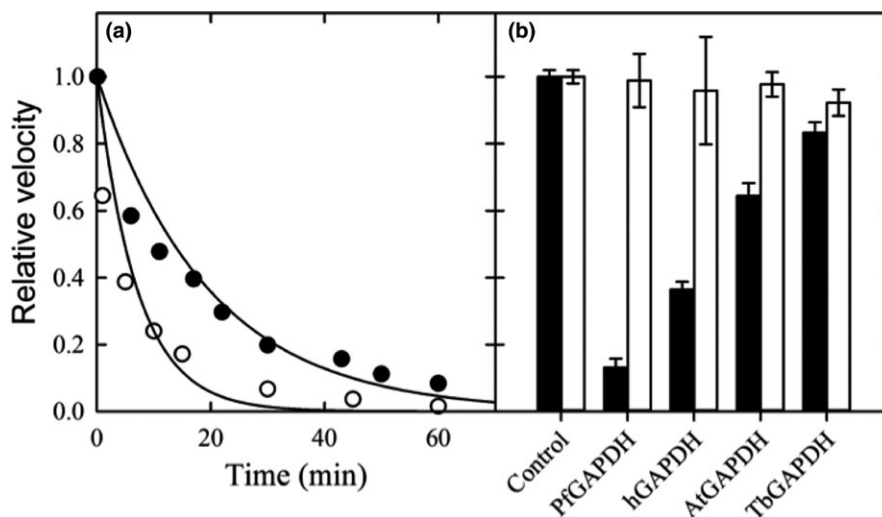
FIGURE 3 (a) Protection of GAPDHs toward **1** inactivation (forward reaction) by the substrate G3P. *Pf*GAPDH was incubated in TEA buffer at pH 7.6 in the presence of 100 μM of **1** (closed squares) or 100 μM of **1** + 5 mM G3P (open circles). Both incubation and enzyme assays were carried out at 25°C. The solid lines represent a fitting of the experimental points to exponential decays. (b) Inhibition of **1** (100 μM) on the reduction in BPGA (reverse reaction) by GAPDH orthologs in the presence of NADH. Residual reactivities were monitored after 15 min of incubation with **1** in TEA buffer at pH 7.6 (black bars). The presence of a BPGA-generating system (3 mM 3-phosphoglycerate, 5 units/ml of 3-phosphoglycerate kinase, and 2 mM ATP) during incubation with **1** protected the enzyme from inactivation almost completely within 15 min (white bars). Both incubation and enzyme assays were carried out at 25°C. The error bars represent the standard deviation of three replicates
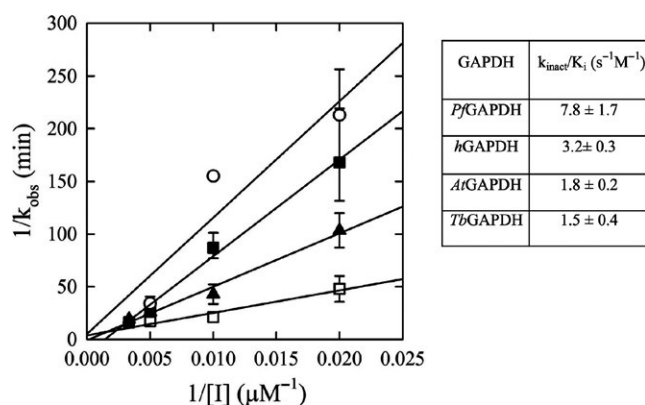

FIGURE 4 Kitz–Wilson double reciprocal plots of the inhibition of *Pf*GAPDH (open squares), *h*GAPDH (closed triangles), *At*GAPDH (closed squares), and *Tb*GAPDH (open circles) by **1** in the 50–300 μM concentration range. Incubation was carried out in TEA buffer, pH 7.6. Both incubation and enzyme assays were carried out at 25°C. The solid lines represent a linear fitting to the experimental points. The error bars represent the standard error of at least two replicates

(and not the catalytic one) has been reported. Therefore, the monoalkylation observed in mass spectrometry (vide infra) further suggests that the alkylated cysteine is indeed the catalytic one.

3.2 | Dialysis studies on *h*GAPDH-1 complex

To determine whether the observed time-dependent inhibition is irreversible, we performed dialysis studies. In the case of irreversible inhibition, the dialysis of the enzyme–inhibitor

mixture should fail to free the enzyme from the inhibitor and to restore the enzymatic activity. Indeed, the irreversibility of the binding of **1** was demonstrated by incubating *h*GAPDH with 200 μM **1** in TEA buffer, pH 7.6, for 2 hr at 20°C, until full inhibition was achieved. Extensive dialysis against **1**-free TEA-buffered solutions for 5 hr at 4°C did not bring about any recovery in activity. Control enzyme solutions subjected to all steps in the absence of **1** showed minimal loss in activity (Figure S3), indicating that the proteins do not undergo significant non-specific inactivation during the procedure. These data are consistent with evidence from previous dilution studies[32] and, overall, support an irreversible inhibition.

3.3 | Kitz–Wilson analysis of inhibition kinetics

The inhibition time–courses were analyzed as Kitz–Wilson double reciprocal plots (Figure 4), which describe the dependence of the reaction rates on the concentration of inhibitor for irreversible inactivation.[37] The reaction parameters were determined by fitting the dependencies to Equation 1.

$$k_{\mathrm{obs}} = \frac{k_{\mathrm{inact}}[I]}{K_i + [I]} \qquad (1)$$

The y-intercept affords the k_{inact}, the maximum rate of inactivation at saturating concentration, whereas the slope gives the k_{inact}/K_i ratio, the apparent second-rate constant of inactivation. Higher k_{inact}/K_i values indicate higher inhibitory potency. The calculated k_{inact}/K_i ratios (see the table of Figure 4) confirmed that **1** reacted fivefold more efficiently

with PfGAPDH (7.8 ± 1.7 M^{-1} s^{-1}) than with the *Arabidopsis* (1.8 ± 0.2 M^{-1} s^{-1}) and *Trypanosoma* (1.5 ± 0.4 M^{-1} s^{-1}) orthologs and twice as efficiently as with the human protein (3.2 ± 0.3 M^{-1} s^{-1}). The poor data on *Tb*GAPDH reflected its tendency to precipitate over time. The zero intercepts indicated that the formation of a non-covalent complex did not significantly contribute to inhibition before the covalent modification, making the formation of the covalent bond the only mechanism of inhibition.[37] The selectivity of irreversible inhibitors depends both on the non-covalent binding to the target (K_i) and the rate at which it reacts with the target after it is bound (k_{inact}), with examples of inhibitors achieving selectivity exploiting either one of the two drivers or both.[41] The optimization of the k_{inact} for lead compounds is usually difficult when the target nucleophile, as in the case of the catalytic cysteine of GAPDHs, is conserved across homologs, limiting the possibility to discriminate, for instance, between the protozoal isoforms and the host (human) isoform. However, here we showed that, despite a negligible contribution of the non-covalent complex in the inhibition mechanisms, **1** could be the starting point for the design of inhibitors that are selective from a kinetic point of view, that is, based on the different rate of the covalent bond formation.

3.4 | Reaction kinetic studies on model thiol

The biochemical data lent enough experimental support to the initial idea that **1** acts as an electrophilic warhead, reacting irreversibly with the GAPDH catalytic cysteine to form a covalent bond. In principle, it can occur via two possible chemical mechanisms:[32] (i) a 1,4-Michael addition and subsequent oxidation of the intermediate hydroquinone, with formation of the corresponding thioether-substituted quinone and (ii) a substitution reaction with phenolate displacement (Figure 5). Both the sulfur addition and substitution reaction to quinones have been thoroughly explored. For instance, natural 2-methyl-1,4-naphthoquinone (menadione) was

found to covalently bind to the cysteine residue of human oxyhemoglobin via the 1,4-Michael-type of thiol addition to quinones.[42] However, the fact that the displacement of leaving groups by sulfur nucleophiles is a common method for the synthesis of thioethers,[43] together with the presence of a good leaving group (phenoxy) in position 2 of **1**, pointed to the substitution reaction as the more plausible one. In fact, in the case of quinones carrying a substituent acting as a leaving group and with a minimal steric hindrance, it has been reported that the position of attack of a sulfur nucleophile occurs at the site of the quinone substituent, giving rise to an ipso substitution product.[43,44] Thus, the presence of the 2-phenoxy leaving group should make **1** more prone to substitution reaction, rather than S-arylation, which are widely described for unsubstituted 1,2-naphthoquinone[45] and 1,4-benzoquinone.[13] Under this hypothesis, the reactivity of **1** against a model thiol was investigated by reaction kinetic studies. The rate constant for the reaction between **1** and (odorless) dodecanthiol in methanol was measured by following the formation of the thioether 2-dodecylthio-1,4-naphthoquinone (**5** in Figure 6) by UV–vis spectroscopy. When **1** was mixed with an excess of dodecanthiol (~15 eq), the typical absorption band of **5** at 413 nm increased during the reaction following a first-order kinetic rate (see Figure 6). As the ipso substitution product is itself a quinone, we did not observe the formation of the hydroquinone **A**, neither the oxidized Michael adduct **B**, both resulting from reaction I (Figure 5). In fact, when monitoring the reaction by ESI-MS, only two major ions were detected corresponding to **1** and the substitution product **5** (see Figure S4).

At the end of the reaction, the recorded spectrum was superimposable to that of an authentic sample of **5**, purposely synthesized (see the Chemistry section in the Supporting Information) to clarify the formation of such adduct. In particular, the rate constants were found to depend on the square root of the concentration of dodecanthiol. A reaction order of 0.5 could be explained considering that the nucleophilic
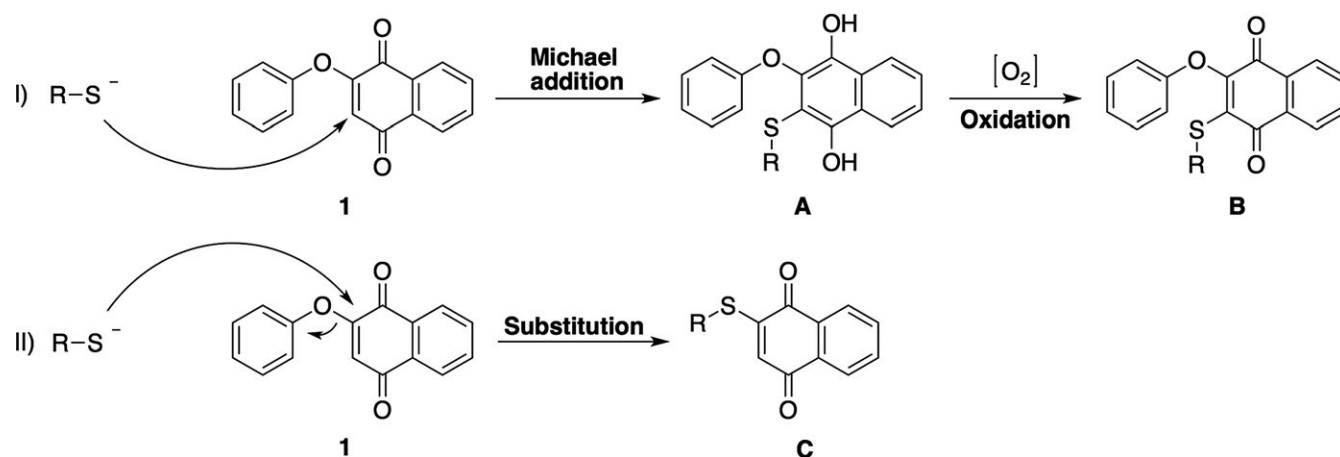

FIGURE 5 Possible mechanisms by which **1** can act as an electrophilic warhead and react irreversibly with thiolates to form a covalent bond
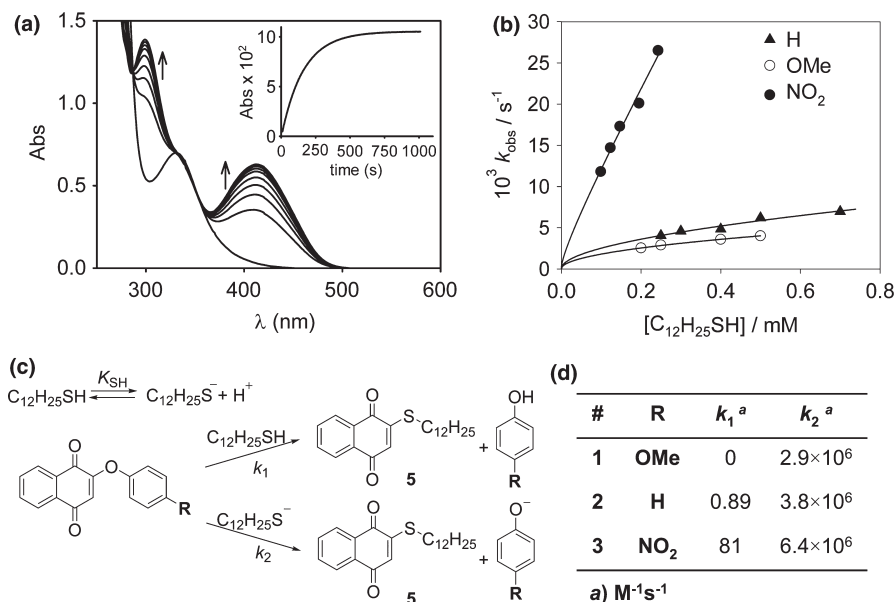
FIGURE 6 Measure of the rate constants for the reaction between substituted phenoxy-naphthoquinones **1–3** and a model thiol in MeOH at 25°C, studied by UV–vis spectrometry. (a) Evolution of the UV–vis spectrum of **1** and $C_{12}H_{25}SH$ (both 2.4×10^{-4} M) recorded every 180 s. The inset shows the absorption at 413 nm as a function of time after mixing **1** (3.4×10^{-5} M) with an excess of thiol (5.0×10^{-4} M).[50] (b) Observed rate constants for the reaction between **1–3** and $C_{12}H_{25}SH$ as a function of thiol concentration. The solid lines represent a fitting to the experimental points based on the scheme. (c) $K_{SH} = 4.0 \times 10^{-15}$ M. (d) Rate constants for the reaction of protonated (k_1) and deprotonated (k_2) thiol with **1–3**, obtained from the fittings. The results are the mean of two independent determinations that varied less by 10%

specie is the thiolate, which is formed in a pre-equilibrium step, as shown in the scheme of Figure 6. This hypothesis is in agreement with the fact that in MeCN, which is a poorer ionizing solvent than MeOH, the reaction does not occur (data not shown). This is also consistent with the notion that cysteine in GAPDH is present in a pK_a-lowering microenvironment[8,46] and, at physiological pH, the corresponding thiol group exists in the highly reactive nucleophilic thiolate state.[6]

Along the lines of reasoning of a substitution mechanism, we envisaged that the reaction kinetics of different 2-phenoxy-1,4-naphthoquinones with dodecanthiol should be influenced by the nature of the leaving group in position 2. Accordingly, we tested the reactivity of derivatives **2**[31] and **3** carrying a 4-methoxyphenoxy or a 4-nitrophenoxy substituent, respectively. As expected, the rate constant (**3 > 1 > 2**) increases in the case of **3** carrying an electron-withdrawing substituent (better leaving group), with respect to the unsubstituted **1**, and to **2**, carrying an electron-donating substituent (worse leaving group). Notably, in the case of **3**, the magnitude of k_1 might suggest a potential reactivity also toward undissociated thiols.

3.5 | Mass spectrometry studies of *Pf*GAPDH-1 complex

We previously failed to detect alkylation of *Tb*GAPDH by mass spectroscopy,[32] mainly because of its instability.

Therefore, MALDI-TOF analysis of undigested *Pf*GAPDH was performed. The measured molecular mass of $39,950 \pm 10$ Da was consistent with the loss of the initial methionine (expected molecular monoisotopic mass: 40,081.21 Da).[14] Upon incubation of 200 μM of **1**, a mass shift of around 145 ± 15 Da was observed, suggesting that a single fragment of 1,4-napthquinone (157 Da) was attached (Figure 7). The shift was consistent with a monoalkylation of each subunit, ruling out non-selective reactivity with other solvent-exposed cysteine residues. This observation suggested that **1** can react with the catalytic thiolate nucleophilic group of the GAPDH cysteine through mechanism II (vide supra). As a matter of fact, mechanism I would have resulted in a larger m/z shift (+250 Da for I versus +157 Da for II). We also failed to detect any m/z shift upon tryptic digestion of any GAPDH upon incubation, possibly because of the limited stability of the adduct in the condition used for MALDI spectrometry. This experiment would have allowed to conclusively identifying the catalytic cysteine as the reactive residue.

3.6 | 1-derived chemical probes

To further probe how the presence/absence of a good leaving group could affect the enzymatic activity and molecular mechanism of action, a properly designed analog (**4**) was synthesized. In particular, in position 2, the phenol of **1** was replaced by an aniline moiety. Importantly, as the aniline
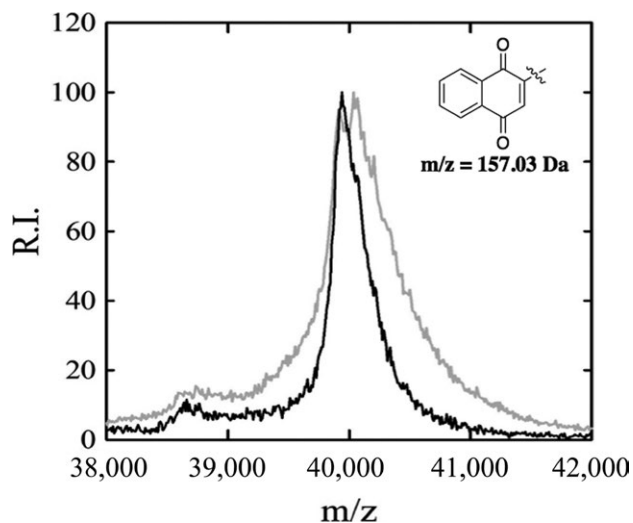
FIGURE 7 Mass spectra of the single charged peak of undigested *Pf*GAPDH (black line) and upon incubation for 2 hr with **1** at 200 μM concentration (gray line). A difference of 145 ± 15 Da is consistent with a monoalkylation by **1**. The sample was diluted 1:10 with HCCA 20 mg/ml in 75% acetonitrile and 2.5% TFA. The *y*-axis is the percent relative intensity of the signal

moiety does not act as a leaving group, it should negatively affect the reactivity of **4** against cysteine nucleophiles. In addition, as a non-reactive analog, **4** might provide clues into the initial non-covalent interaction of **1**. This is because **4** is the corresponding isoster of **1**, sharing, in principle, most of the binding interactions with the enzyme. As expected, **4** did not produce significant inhibition on GAPDHs. Considering that **4** behaves as a non-reactive analog of **1**, we investigated the possibility that it might act as a non-covalent inhibitor at high concentrations. However, even at 200 μM concentration in the assay mixture, it did not bring about a meaningful inhibition for *Pf*GAPDH, the most reactive of the orthologs (Figure S5), suggesting that the contribution for inhibition of a non-covalent binding before the covalent reaction takes place is small (also supported by the Kitz–Wilson analysis). In addition, **4** did not display any inhibitory activity against *At*GAPDH up to a concentration of 50 μM, which was instead inhibited by 40% by **1** at 10 μM. A similar behavior was observed for *h*GAPDH (24% for **4** versus 100% for **1**) and *Tb*GAPDH (20% for **4** versus 100% for **1**) at 10 μM.

With regard to **2** (Figure 6) and analogs[31] carrying different leaving groups in position 2, we previously proposed that their inhibitory activities were correlated with both the possibility of properly interacting with the catalytic cysteine and with their susceptibility to the subsequent nucleophilic substitution reaction.[31] In this respect, docking studies demonstrated that steric hindrance is a major determinant affecting the correct positioning within the GAPDH active site.[31] Indeed, **3**, (Figure 6), bearing the 4-nitro-phenoxy substituent, displayed only 37% of inhibition against *Tb*GAPDH (versus 100% for **1**) at 10 μM. Thus, this lower inhibitory activity does not seem correlated with the presence of a better leaving group, rather to the fact that the bulky nitro group of **3** creates steric hindrance. Conversely, **3** was the most effective in the reaction kinetic studies, where steric concern is not present.

3.7 | Whole-cell studies

We performed experiments to evaluate **2**–**4** in a cellular context (*Tb* and *Pf* parasites, and L6 cells) in comparison with **1** (Table 1). In the case of *T. brucei*, the rank in antitrypanosomal activity perfectly matched that of GAPDH inhibition (**1** > **3** > **2** > **4**). This is not the case for the antiplasmodial activity, though. In fact, **4**, which did not show any significant *Pf*GAPDH inhibitory activity, turned out to be a submicromolar inhibitor of the parasite growth, suggesting an alternative mechanism of action, in addition to GAPDH inhibition. Indeed, we demonstrated that **1**, thanks to its quinone structure, was also able to generate oxygen radicals, a mechanism that additionally contributes to its antiparasitic activity.[32]

3.8 | Activity of 1 toward cysteine proteases

1–**3** all share the highly reactive 2-phenoxynaphthoquinone scaffold, which, in principle, is prone to unspecific covalent reactions with other protein thiols. Given the increased attention paid to the so-called PAINS (pan-assay interference compounds),[47] a further discussion of **1** in relationship to covalent modifiers as PAINS compounds is warranted. The ability of the 2-phenoxyquinone moiety to act as a warhead can cause **1** and analogs to act as frequent hitters in screening assays due to interference, rather than via specific interactions with the intended biological targets. In particular, the possibility that the inhibition is more affected by the chemical reactivity of the naphthoquinone moiety rather than a specific molecular recognition should be definitively ruled out. This concern is quite important considering that the intrinsic chemical reactivity of naphthoquinones **1**–**3** could be a potential limitation to their applicability in a biological context, where other thiol species are expected to occur at high concentrations (e.g., glutathione). This is not only a concern for drug discovery, but also for chemical biology. Indeed, to this end, we preliminarily tested the inhibitory activity of **1** against two cysteine proteases sharing with GAPDH the histidine–cysteine catalytic dyad, that is, human caspase-3 and cathepsin B. In particular, whereas caspase-3 shows a pK_a of 6.6,[48] cathepsin B has a very nucleophilic active-site cysteine (pK_a = 3.4)[49] that can more readily react with thiol-modifying reagents. Notably, when tested at a concentration of 10 μM, which approximates the IC_{50} of **1** toward

*Tb*GAPDH (IC$_{50}$ = 7.25 μM),[32] against human cathepsin B and caspase-3, we could not detect any significant inhibition (see Supporting Information). Thus, it appears that the selective reaction of **1** with the catalytic cysteine of GAPDH is not because the enzyme provides an exceptionally good nucleophile, and is not solely due its ability to act as an optimal leaving group.

4 | CONCLUSIONS

GAPDHs are inhibited by 2-phenoxy-1,4-naphthoquinone compounds through the irreversible monoalkylation of each subunit with a phenolate displacement mechanism. The inhibition kinetics indicated that the formation of non-covalent complexes does not contribute significantly to inhibition, which appears solely associated with the formation of covalent bond. However, GAPDH homologs exhibited markedly different reaction rates, suggesting that the microenvironment of the catalytic cysteine significantly affects their reactivity. Two cysteine proteases tested as control were not inhibited by 2-phenoxy-1,4-naphthoquinone, suggesting its potential selectivity toward GAPDH within the cysteine-dependent enzymes. 2-Phenoxy-1,4-naphthoquinone and its analogs showed in vivo antitrypanosomal and antiplasmodial activities at submicromolar concentrations. Overall, despite the moderate potency, the 2-phenoxy-1,4-naphthoquinone scaffold can be regarded as "warhead" starting fragment for the identification of further inhibitors with increased potency and selectivity. By fine-tuning the inherent chemical reactivity and exploiting the kinetic reactivities of different isoforms, it should be possible to tailor them to a variety of GAPDH isoforms that are promising therapeutic targets, particularly selecting analogs that are significantly more reactive toward parasitic orthologs in comparison with the human form.

CONFLICT OF INTEREST

The authors declare no conflict of interest.

AUTHOR CONTRIBUTIONS

The manuscript was written through contributions of all authors. All authors have given approval to the final version of the manuscript.

REFERENCES

[1] H. L. Segal, P. D. Boyer, *J. Biol. Chem.* **1953**, *204*, 265.

[2] D. R. Trentham, *Biochem. J.* **1971**, *122*, 71.

[3] D. R. Trentham, *Biochem. J.* **1971**, *122*, 59.

[4] N. W. Seidler, *Adv. Exp. Med. Biol.* **2013**, *985*, 37.

[5] S. Moniot, S. Bruno, C. Vonrhein, C. Didierjean, S. Boschi-Muller, M. Vas, G. Bricogne, G. Branlant, A. Mozzarelli, C. Corbier, *J. Biol. Chem.* **2008**, *283*, 21693.

[6] C. J. Martyniuk, B. Fang, J. M. Koomen, T. Gavin, L. Zhang, D. S. Barber, R. M. LoPachin, *Chem. Res. Toxicol.* **2011**, *24*, 2302.

[7] A. K. Tummanapelli, S. Vasudevan, *J. Phys. Chem. B* **2015**, *119*, 15353.

[8] M. Zaffagnini, S. Fermani, A. Costa, S. D. Lemaire, P. Trost, *Front Plant Sci.* **2013**, *4*, 450.

[9] S. M. Marino, V. N. Gladyshev, *J. Biol. Chem.* **2012**, *287*, 4419.

[10] E. C. Campian, J. Cai, F. W. Benz, *Chem. Biol. Interact.* **2002**, *140*, 279.

[11] E. C. Dietze, A. Schafer, J. G. Omichinski, S. D. Nelson, *Chem. Res. Toxicol.* **1997**, *10*, 1097.

[12] D. S. Choi, Y. B. Kim, Y. H. Lee, S. H. Cha, D. E. Sok, *Cell Biol. Toxicol.* **1995**, *11*, 23.

[13] C. E. Rodriguez, J. M. Fukuto, K. Taguchi, J. Froines, A. K. Cho, *Chem. Biol. Interact.* **2005**, *155*, 97.

[14] S. Bruno, A. Pinto, G. Paredi, L. Tamborini, C. De Micheli, V. La Pietra, L. Marinelli, E. Novellino, P. Conti, A. Mozzarelli, *J. Med. Chem.* **2014**, *57*, 7465.

[15] S. Bruno, M. Margiotta, A. Pinto, G. Cullia, P. Conti, C. De Micheli, A. Mozzarelli, *Bioorg. Med. Chem.* **2016**, *24*, 2654.

[16] S. Song, T. Finkel, *Nat. Cell Biol.* **2007**, *9*, 869.

[17] E. Jortzik, K. Becker, in Apicomplexan Parasites: Molecular Approaches toward Targeted Drug Development, (Ed.: K. Becker), Wiley-VCH Verlag GmbH & Co. KGaA, Weinheim, Germany **2011**, pp. 75–95.

[18] M. Gualdrón-López, P. A. M. Michels, W. Quiñones, A. J. Cáceres, L. Avilán, J.-L. Concepción, in Function of Glycosomes in the Metabolism of Trypanosomatid Parasites and the Promise of Glycosomal Proteins as Drug Targets, (Eds: T. Jäger, O. Koch, L. Flohé), Wiley-VCH Verlag GmbH & Co. KGaA, Weinheim, Germany **2013**, pp. 121–151.

[19] X. Barros-Alvarez, M. Gualdron-Lopez, H. Acosta, A. J. Caceres, M. A. Graminha, P. A. Michels, J. L. Concepción, W. Quiñones, *Curr. Med. Chem.* **2014**, *21*, 1679.

[20] A. Leitao, A. D. Andricopulo, G. Oliva, M. T. Pupo, A. A. de Marchi, P. C. Vieira, M. F. G. da Silva, V. F. Ferreira, M. C. B. de Souza, M. M. Sá, V. R. Moraes, *Bioorg. Med. Chem. Lett.* **2004**, *14*, 2199.

[21] R. V. Guido, G. Oliva, C. A. Montanari, A. D. Andricopulo, *J. Chem. Inf. Model.* **2008**, *48*, 918.

[22] F. V. Maluf, A. D. Andricopulo, G. Oliva, R. V. Guido, *Future Med. Chem.* **2013**, *5*, 2019.

[23] F. C. Herrmann, M. Lenz, J. Jose, M. Kaiser, R. Brun, T. J. Schmidt, *Molecules* **2015**, *20*, 16154.

[24] R. F. Freitas, I. M. Prokopczyk, A. Zottis, G. Oliva, A. D. Andricopulo, M. T. Trevisan, W. Vilegas, M. G. V. Silva, C. A. Montanari, *Bioorg. Med. Chem.* **2009**, *17*, 2476.

[25] A. J. Caceres, P. A. M. Michels, V. Hannaert, *Mol. Biochem. Parasit.* **2010**, *169*, 50.

[26] S. Ganapathy-Kanniappan, J. F. H. Geschwind, *Mol. Cancer.* **2013**, *12*, 152.

[27] C. Granchi, D. Fancelli, F. Minutolo, *Bioorg. Med. Chem. Lett.* **2014**, *24*, 4915.

[28] A. Tarze, A. Deniaud, M. Le Bras, E. Maillier, D. Molle, N. Larochette, N. Zamzami, G. Jan, G. Kroemer, C. Brenner, *Oncogene* **2007**, *26*, 2606.

[29] D. Zala, M. V. Hinckelmann, H. Yu, M. M. Lyra da Cunha, G. Liot, F. P. Cordelieres, S. Marco, F. Saudou, *Cell* **2013**, *152*, 479.

[30] M. L. Bolognesi, F. Lizzi, R. Perozzo, R. Brun, A. Cavalli, *Bioorg. Med. Chem. Lett.* **2008**, *18*, 2272.

[31] F. Prati, C. Bergamini, M. T. Molina, F. Falchi, A. Cavalli, M. Kaiser, R. Brun, R. Fato, M. L. Bolognesi, *J. Med. Chem.* **2015**, *58*, 6422.

[32] S. Pieretti, J. R. Haanstra, M. Mazet, R. Perozzo, C. Bergamini, F. Prati, R. Fato, G. Lenaz, G. Capranico, R. Brun, B. M. Bakker, P. A. Michels, L. Scapozza, M. L. Bolognesi, A. Cavalli, *Plos Neglect. Trop. Dis.* **2013**, *7*, e2012.

[33] F. Belluti, E. Uliassi, G. Veronesi, C. Bergamini, M. Kaiser, R. Brun, A. Viola, R. Fato, P. A. Michels, R. L. Krauth-Siegel, A. Cavalli, M. L. Bolognesi, *ChemMedChem* **2014**, *9*, 371.

[34] M. Bedhomme, M. Adamo, C. H. Marchand, J. Couturier, N. Rouhier, S. D. Lemaire, M. Zaffagnini, P. Trost, *Biochem. J.* **2012**, *445*, 337.

[35] M. M. Bradford, *Anal. Biochem.* **1976**, *72*, 248.

[36] W. Ferdinand, *Biochem. J.* **1964**, *92*, 578.

[37] R. Kitz, I. B. Wilson, *J. Biol. Chem.* **1962**, *237*, 3245.

[38] I. Orhan, B. Sener, M. Kaiser, R. Brun, D. Tasdemir, *Mar. Drugs* **2010**, *8*, 47.

[39] M. S. Castilho, F. Pavao, G. Oliva, S. Ladame, M. Willson, J. Perie, *Biochemistry* **2003**, *42*, 7143.

[40] O. Daltrop, S. J. Ferguson, *J. Biol. Chem.* **2004**, *279*, 45347.

[41] J. Singh, R. C. Petter, T. A. Baillie, A. Whitty, *Nat. Rev. Drug Discov.* **2011**, *10*, 307.

[42] W. W. Li, J. Heinze, W. Haehnel, *J. Am. Chem. Soc.* **2005**, *127*, 6140.

[43] J. Clayden, P. MacLellan, *Beilstein J. Org. Chem.* **2011**, *7*, 582.

[44] A. Wissner, M. B. Floyd, B. D. Johnson, H. Fraser, C. Ingalls, T. Nittoli, R. G. Dushin, C. Discafani, R. Nilakantan, J. Marini, M. Ravi, K. Cheung, X. Tan, S. Musto, T. Annable, M. M. Siegel, F. Loganzo, *J. Med. Chem.* **2005**, *48*, 7560.

[45] T. Miura, H. Kakehashi, Y. Shinkai, Y. Egara, R. Hirose, A. K. Cho, Y. Kumagai, *Chem. Res. Toxicol.* **2011**, *24*, 1836.

[46] M. Zaffagnini, S. Fermani, M. Calvaresi, R. Orru, L. Iommarini, F. Sparla, G. Falini, A. Bottoni, P. Trost, *Antioxid. Redox Signal.* **2016**, *24*, 502.

[47] J. B. Baell, *Future Med. Chem.* **2010**, *2*, 1529.

[48] P. Karki, J. Lee, S. Y. Shin, B. Cho, I. S. Park, *Arch. Biochem. Biophys.* **2005**, *442*, 125.

[49] S. Hasnain, T. Hirama, A. Tam, J. S. Mort, *J. Biol. Chem.* **1992**, *267*, 4713.

[50] J. F. Bunnett, L. A. Retallick, *J. Am. Chem. Soc.* **1967**, *89*, 423.

SUPPORTING INFORMATION

Additional Supporting Information may be found online in the supporting information tab for this article.